Pena, L. D., Goldstein, S. L., Hemming, S. R., Jones, K. M., Calvo, E., Pelejero, C. and Cacho, I., Rapid changes in meridional advection of Southern Ocean intermediate waters to the tropical Pacific during the last 30 kyr.

Supplementary Material:

Supplementary Material Contents:

S1. Figure S1. Present-day water mass characteristics for WTA cores with shallow to intermediate ε_{Nd} records.

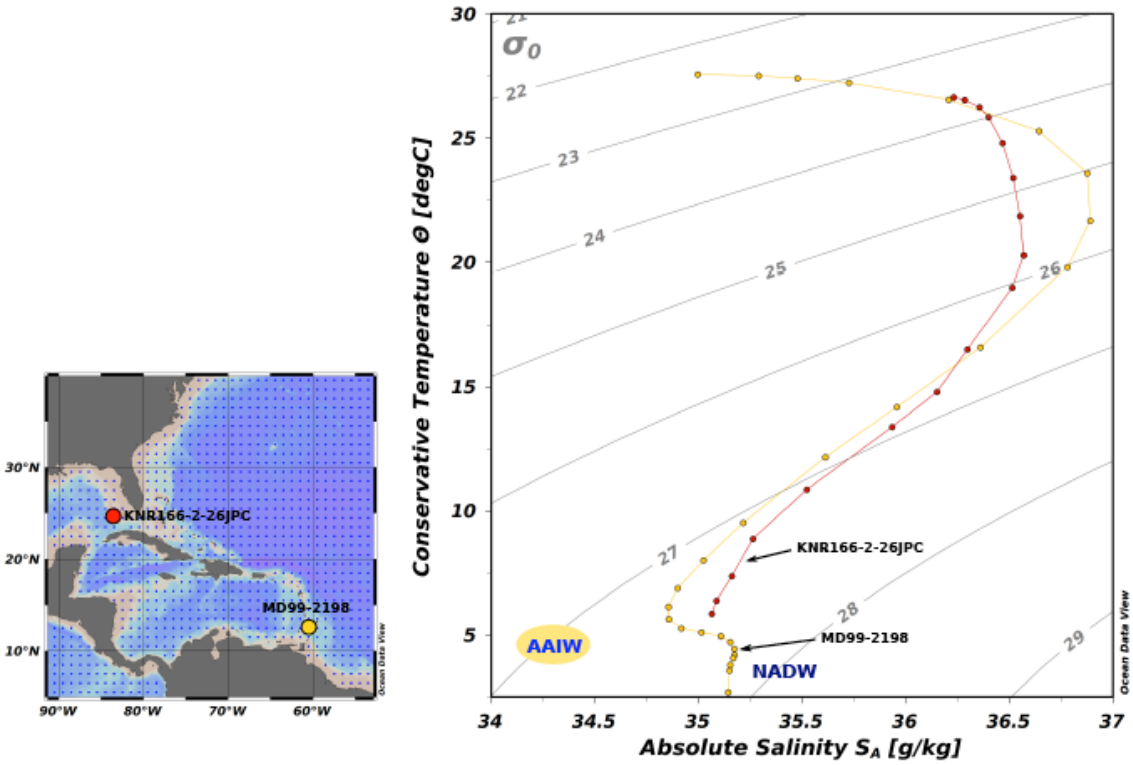

Fig. S1 caption: Conservative temperature *(Θ)* versus absolute salinity *(S_A)* for the water columns at WTA sites of cores with shallow to intermediate depth ε_{Nd} records from the LGM to today. Potential density *(σ_0)* isopycnals are also shown. In the text, the ODP Site 1240 ε_{Nd} data are compared to records from core MD99-2168, from the Tobago Basin at an intermediate depth of 1330 m (Pahnke et al. 2008), and core KNR166-2-26JPC, from the Gulf of Mexico at a relatively shallow depth of 546 m (Xie et al. 2012). The Θ-S_A compositions of AAIW and NADW are from the World Ocean Atlas 2009 (WOA09, Antonov et al. 2010; Locarnini et al. 2010), and represent estimates of annual Θ and S_A for 1° longitude-latitude squares at set depths at the core locations. The compositions of the AAIW end-member, and NADW in the WTA, are shown. The arrows point to the compositions of the bottom waters at the core depths.

S2. Comparison of the Tobago Basin and the Gulf of Mexico records.

Both the Tobago Basin (Pahnke et al., 2008) and the Gulf of Mexico (Xie et al., 2012) studies conclude that their records show changes in AAIW over time (Fig. 4b), but they draw opposite conclusions. Further studies will determine which interpretation is the better one. In the meantime, we favor the Tobago Basin interpretation by Pahnke et al. (2008), and in the text we compare the history of intermediate waters in the EUC to the WTA based on their conclusions, for the reasons given below.

The Tobago Basin record (Fig. 4b) shows excursions to more positive ε_{Nd} values during HS1 and YD (ε_{Nd} ~ -9.5), compared to the late-LGM, B-A, and PB (ε_{Nd} ~ -11 to -12). Pahnke et al. (2008) interpret these changes as indicating stronger AAIW signals at the site during H1 and YD, displacing NADW or GNAIW, which is stronger in the late-LGM, B-A, PB, and Holocene. The Gulf of Mexico record also shows excursions during HS1 and YD (also to ε_{Nd} ~ -9.5), but to more negative ε_{Nd} values compared to late-LGM, B-A, and PB, when (ε_{Nd} ~ -9 or ~-8 to -8.5). Xie et al. (2009) interpret these changes as indicating a stronger GNAIW signals during H1 and YD, displacing AAIW, during the late-LGM, B-A, PB, and Holocene.

If Xie et al. (2012) are correct, then AAIW, only slightly modified from its original composition in the Southern Ocean, must be the dominant water mass at this Gulf of Mexico site during the LGM, B-A, PB, and Holocene. Figure S1 shows that the Θ-S_A characteristics at the site are both much warmer (~3°C) and saltier (~1‰) than AAIW. This means that any AAIW that has arrived at the site has been significantly diluted by other water masses, to the extent that there is little indication left of AAIW characteristics. These considerations are difficult to reconcile with the assumption by Xie et al. (2009) that the ε_{Nd} values in the recent part of the record are dominated by AAIW. More likely, the typical Holocene ε_{Nd} values of ~ -8.5 at the Gulf of Mexico site reflect regional sources of Nd. In this context, a study of surface soil samples from Florida show ε_{Nd} values between -5.6 and -10.5 (Kamenev et al. 2009), and Goldstein and Jacobsen (1987) report ε_{Nd} = -8.5 on a Mississippi river water sample, all of which are consistent with a regional source of Nd at this relatively shallow site.

The interpretation of Pahnke et al. (2008) is easier to reconcile with the water mass characteristics at the Tobago Basin site (Fig. S1). In the present-day the dominant water mass is modified NADW, which is reflected by low Holocene ε_{Nd} values between ~ -10 and -12, significantly more negative than AAIW. Going back in time to glacial times, there is strong evidence (Rutberg et al. 2000, Foster et al. 2007, van de Flierdt et al. 2006) that the overall ε_{Nd} values of North Atlantic source waters remained similar to today (although excursions over short time scales are not precluded). The water column profile at the site location shows that, toward shallower depths, the Θ-S_A line curves toward lower salinity and toward the AAIW end-member. This clearly indicates the presence of modified AAIW in the water column above the Tobago Basin site (in contrast to the Gulf of Mexico site), which we reasonably assume to have more positive ε_{Nd} values (in the absence of any data yet published from the area). The ε_{Nd} excursions observed by Pahnke et al. (2008) during the HS1 and YD, toward more positive ε_{Nd} values, are thus most simply interpreted as indicating stronger incursions of AAIW at the depths of the core site.

Finally, it is interesting that during the HS1 and YD events, the Tobago Basin and the Gulf of Mexico profiles show excursions to the same values ε_{Nd} values of ~ -9.5 (Fig. 4b). This may indicate that both records are observing the same stronger signal of AAIW, consistent with the interpretation of Pahnke et al. (2008).

S3. Figure S2. Illustration of EEP-SOIW mixing systematics

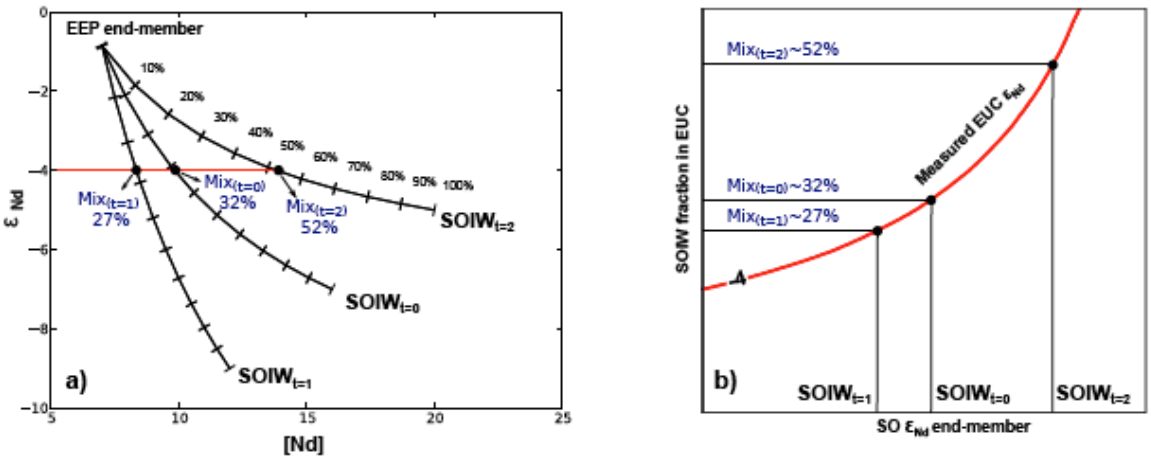

Fig. S2 caption. a) Illustration of the mixing relationships between 3 different SOIW end-members and the (constant) EEP end-member. The diagram illustrates the scenario where the same ε_{Nd} value (here -4) is measured in our Site 1240 samples at three different points in time (t=0, 1, and 2) characterized by three different compositions for the SOIW end-member. The figure shows how the fraction of SOIW is markedly different (here varying between 27% and 52%) in each case. b) Illustration the same calculation as in S2a, showing the changes in the SOIW fraction in the EUC as the ε_{Nd} of the SOIW end-member varies. These diagrams illustrate the considerations that went into creating Fig. 4c,d in the text (Fig. 4 a,b, is analogous but assumes the same [Nd] through time in the SOIW end-member). The way we determine the SOIW end-member is explained in Section S5.

S4. Table S1: Present-day water mass end-member values for mixing calculations

Water masses	[Nd] (pmol/kg)	ε_{Nd}	Reference
PDW	40	-4	(Piepgras and Wasserburg, 1980, Piepgras and Jacobsen, 1987)
CDW	26.5	-8	(Piepgras and Wasserburg, 1982, Carter et al., 2012)
NADW	17	-13.5	(Piepgras and Wasserburg, 1980, 1987)
EEP	7	-0.85[1]	(This study, Lacan and Jeandel, 2001)
SOIW	17	-6 to -7	(German et al., 1995, Carter et al., 2012)

[1]Calculated based on a 5% contribution of SOIW waters in the EUC, as explained in the text.

S5. Estimation of SOIW advection into the EUC

In Figures 5, 6c we estimate the fraction of SOIW in the EUC through time, thus illustrating the relative changes in the advection of SOIW to the EUC using a two end-member mixing model. Given two water mass end-members with known Nd concentrations [Nd] and ε_{Nd} values, we construct a mixing line (Fig S2a) using standard mixing equations:

$$[Nd]_m = [Nd]_1 * f_1 \quad + \quad [Nd]_2 * (1 - f_1) \qquad (1)$$

and

$$(e_{Nd})_m = \frac{(e_{Nd})_1 * [Nd]_1 * f_1 \quad + \quad (e_{Nd})_2 * [Nd]_2 * (1 - f_1)}{[Nd]_1 * f_1 \quad + \quad [Nd]_2 * (1 - f_1)} \qquad (2)$$

where *[Nd]* is the concentration of Nd, ε_{Nd} is the Nd isotope ratio, and *1, 2, m* represent the two end-members and the mixture, respectively. Thus, by assuming that ε_{Nd} in our ODP Site 1240 samples reflect mixing between SOIW and EEP waters, we can estimate the relative contributions of each. However, if one of the end-members is not constant through time (in this case SOIW, Figs. 4c, S2), then the same ε_{Nd} value in the EUC at different times can reflect different relative contribution from each end-member. Figure S2a illustrates this situation by showing three mixing lines between the EEP close to Site 1240 and the SOIW end-member at three different time periods (t=0, t=1 and t=2). The three mixing scenarios use the same EEP end-

member (having the same ε_{Nd} and [Nd] value), but different SOIW end-member values (both ε_{Nd} and [Nd]). Figure S2a shows that if we measure ε_{Nd}=-4 in the mixed EUC waters, then the relative contribution to this isotopic signal from the SOIW end-member also changes accordingly (i.e. ranging between 27% and 52% for these three cases).Figure S2b shows, for the same mixing scenarios, the variation in the fraction of the SOIW in the EUC withthe changing SOIW end-member composition.

The calculation assumes that the variability of the Southern Ocean end-member over time is preserved in the authigenic Fe-Mn oxide fractions of core V19-188, which was also used by Pahnke et al. (2008). This core is from the Indian Ocean but the site is bathed in CDW and the core top ε_{Nd} shows Southern Ocean values. Compared to CDW, SOIW is ~1-2 ε_{Nd} units more positive, and ~10 pg/kg of seawater lower in [Nd], and we maintain this difference through time. In the text we present results of two calculations: one calculation assumes that the SOIW ε_{Nd} values change along with V19-188, but [Nd] remains constant (Figs. 5a,b); the other assumes that ε_{Nd} and [Nd] of CDW through time broadly reflects mixing of North Atlantic (NADW) and North Pacific (PDW) end-members, like today, and thus [Nd] varies in CDW and is determined by the NADW-PDW mixture (Figs. 5c,d).

S6. Materials and Methods

As it is critical to remove all of the Fe-Mn coating in the samples in order to measure the Nd bound to the foraminiferal calcite, we have followed the cleaning protocol used for trace element analyses in the same samples (Pena et al., 2005), with some modifications in the volume of the reagents used due to the larger samples. The foraminifera in each sample are gently crushed with two glass slides under a binocular microscope in order to expose the inner surfaces of the foraminifera chambers to the cleaning reagents, because at ODP Site 1240 the Fe-Mn coatings are preferentially located in the inner part of the foraminifera shells (Pena et al., 2005; Pena et al., 2008b). After crushing, clays and small particles are removed using QD water and methanol in an ultrasonic bath. Samples are rinsed until the supernatant is completely clean. Immediately afterward a reductive step removes the Fe-Mn coatings using a 1:4 mixture of hydrazine hydroxide/ammonium citrate (Pena et al., 2005), in a hot water bath at 85-90°C with brief

sonicating periods for about 30 minutes. Next an oxidative cleaning uses a NaOH buffered hydrogen peroxide solution to remove any organic matter. The reaction takes place for 10 minutes in a boiling water bath. The order of these two cleaning steps (reductive-then-oxidative) is critical because during the reductive step insoluble metal sulphides (e.g. CdS) can be formed and precipitate in the sample (Rosenthal et al., 1995). Finally, a weak acid leaching step with diluted HNO_3 is applied to every sample in order to chemically etch off any remaining coating or re-adsorbed elements from the surfaces.

After cleaning, samples are dissolved and two small aliquots separated for trace element and rare earth element (REE) analyses. Separation of Nd for isotope analyses uses standard chromatographic techniques used at LDEO (Eichrom Tru-Spec resin, and α-hydroxyisobutyric acid and cation resin). $\varepsilon_{Nd}$was measured on a VG Sector 54 thermal ionization mass spectrometer at LDEO by dynamic multicollection, as NdO^+, which is more than an order of magnitude more sensitive than running Nd^+ metal, and thus allows for measurement of samples as small as a few nanograms. $^{143}Nd/^{144}Nd$ ratios were mass fractionation corrected to $^{146}Nd/^{144}Nd = 0.7219$ and adjusted to a JNdi-1 value of $^{143}Nd/^{144}Nd = 0.512115$ (Tanaka et al., 2000). External reproducibility from routine runs of the JNdi-1 standards was $^{143}Nd/^{144}Nd = 0.512114 \pm 0.000015$ (2σ, n = 21).

Weighed aliquots of samples for REE concentration analyses (La, Ce, Pr, Nd, Sm, Eu, Gd, Tb, Dy, Ho, Er, Tm, Yb and Lu) were spiked with a multi-element REE spike (^{142}Ce, ^{145}Nd, ^{149}Sm, ^{153}Eu, ^{155}Gd, ^{161}Dy, ^{167}Er and ^{171}Yb). After equilibration for >24 hours, the REEs were separated from the calcite matrix using Eichrom Re-Spec resin. This procedure was designed for use at LDEO using a VG Axiom MC-ICPMS in ion counting mode, whose sensitivity is ~$2.5*10^6$ cps on a one ppb Pr solution. Analyses of REEs on the ICPMS uses a desolvating nebulizer, such as the Cetac Aridus, using nitrogen carrier gas, which ensures that a minimal amount of oxides are formed and thus prevents the need for oxide corrections. Typical oxide formation rates observed during the development of this procedure were 0.008% to 0.015% for a pure Ce solution. Typical internal errors were better than 2%, accounting for error magnification. External reproducibility was monitored with a spiked REE standard solution and was better that 3% for most elements.

Laser ablation analyses of foraminifera shells used a New Wave UP-193-FX laser coupled to a VG PlasmaQuad ExCell quadrupole ICPMS. This excimer laser operates at a low wavelength (193nm), therefore it creates very reproducible laser pits. Routine precision is 1-3%. Spot sizes range from 5 to 150 μm, which is ideal for small foraminifera. The ExCell includes a multipole collision cell to minimize argide interferences in the mid-mass range, and a new off-axis lens system, which has decreased instrument backgrounds to <0.5 cps. It achieves <10 parts per quadrillion (10^{15}) detection limits on ^{238}U.

S7. Table S2. Nd isotope data

Depth (mcd)[a]	Age (ky)	$^{143}Nd/^{144}Nd \pm 2\sigma$[b]	ε_{Nd}	SOIW advection (constant Nd)[c]	SOIW advection (variable Nd)[c]
0.01	1.91	0.512553±09	-1.66	0.057	0.055
0.02	2.05	0.512558±09	-1.56	0.049	0.048
0.21	4.71	0.512574±09	-1.25	0.027	0.027
0.61	7.78	0.512559±08	-1.55	0.051	0.048
0.70	8.41	0.512540±16	-1.91	0.076	0.068
0.90	9.43	0.512498±12	-2.73	0.174	0.151
0.98	9.76	0.512492±26	-2.85	0.183	0.156
1.22	11.07	0.512542±11	-1.87	0.098	0.076
1.41	12.91	0.512580±11	-1.14	0.027	0.020
1.61	13.85	0.512574±09	-1.25	0.036	0.028
1.81	14.93	0.512567±11	-1.38	0.052	0.038
2.01	16.02	0.512544±11	-1.83	0.150	0.090
2.15	16.78	0.512527±21	-2.16	0.155	0.110
2.31	17.33	0.512531±10	-2.08	0.134	0.099
2.41	17.98	0.512514±32	-2.43	0.171	0.131
2.49	18.50	0.512559±14	-1.55	0.067	0.051
2.57	19.02	0.512541±28	-1.89	0.103	0.078
2.63	19.41	0.512524±14	-2.23	0.140	0.109
2.91	20.88	0.512508±11	-2.54	0.178	0.140
2.99	21.29	0.512505±13	-2.59	0.199	0.151
3.12	21.95	0.512546±11	-1.80	0.111	0.076
3.20	22.53	0.512527±14	-2.16	0.181	0.120
3.40	25.28	0.512515±17	-2.39	0.276	0.174
3.60	27.80	0.512538±14	-1.95	0.178	0.107

[a] meters composite depth

[b] Individual run precision of individual analyses ($2\sigma_m$). Absolute errors of $^{143}Nd/^{144}Nd$ have to be multiplied by 10^{-6}. As noted in the Supplementary Materials section Materials and Methods, the reproducibility of the JNdi standard is ±0.000015.

[c] Fraction of the EUC waters composed of SOIW. The calculation is explained in the text, and in the Supplementary Materials section on Estimation of SOIW advection into the EUC.

S8. Table S3. REE/Ca ratios (nmol/mol) measured in ODP Site 1240 planktonic foraminifera.

Sample[a]	La	Ce	Pr	Nd	Sm	Eu	Gd	Tb	Dy	Ho	Er	Tm	Yb	Lu
Clean foraminifera														
1.91	315	235	55.0	229	47.8	13.4	64.5	9.39	67.3	16.6	49.6	7.43	48.5	7.33
2.05	387	283	67.9	275	56.8	16.2	77.3	11.0	80.7	20.0	59.2	8.96	60.7	9.31
7.78	276	179	46.6	192	39.3	11.4	54.4	8.01	55.9	14.1	42.3	6.24	41.8	6.35
9.43	232	133	41.4	169	36.1	10.5	50.2	7.27	53.5	13.3	39.0	6.05	38.4	5.70
10.97	120	73.5	22.3	94.9	20.1	5.93	29.0	4.26	30.8	7.70	23.5	3.68	23.5	3.63
11.08	151	88.1	28.0	118	25.8	7.49	35.5	5.38	39.0	9.67	29.5	4.82	29.0	4.43
12.91	217	150	41.0	168	36.8	10.7	50.6	7.45	54.0	13.2	39.6	6.21	39.9	6.11
14.93	145	114	27.6	115	24.5	7.03	33.9	4.92	35.1	8.70	25.8	3.91	26.7	4.05
16.02	180	147	35.0	149	32.0	9.05	42.9	6.55	45.4	11.1	33.7	4.89	33.8	5.20
17.33	161	119	28.9	123	25.7	7.06	35.6	5.20	36.8	9.29	27.9	4.02	28.2	4.41
17.98	167	114	31.4	136	28.3	7.99	39.4	5.98	41.7	10.3	30.8	4.48	31.6	4.81
19.41	161	115	29.8	124	26.1	7.05	35.9	5.22	37.9	9.41	28.4	4.13	28.7	4.57
20.88	236	164	44.2	187	39.0	10.8	54.4	7.86	56.0	13.9	40.7	5.91	41.8	6.32
Average REE/Ca	211	147	38.4	160	33.7	9.58	46.4	6.81	48.8	12.1	36.2	5.44	36.4	5.55
Unclean foraminifera														
1.91	1555	2872	331	1301	256	54.9	305	33.9	246	45.5	139	17.6	131	14.0
Seawater														
AAIW[b]	1.47	0.304	0.238	0.933	0.177	0.049	0.295	0.057	0.373	0.108	0.383	0.054	0.383	0.065

[a] Sample age in ky.

[b] Antarctic Intermediate Water REE/Ca ratios from German et al., 1995, and using [Ca] = 10.46 mmol/kg.

S9.References cited in the supplementary materials

Antonov, J.I., Seidov, D., Boyer, T.P., Locarnini, R.A. Mishonov, A.V.,Garcia, H.E., Baranova,O.K.,Zweng, M.M., Johnson, D.R., 2010. *World Ocean Atlas 2009, Volume 2: Salinity.* S. Levitus, Ed. NOAA Atlas NESDIS 69, U.S. Government Printing Office, Washington, D.C., 184 pp.

Carter, P., Vance, D., Hillenbrand, C.D., Smith, J., Shoosmith, D., 2012. The neodymium isotopic composition of waters masses in the eastern Pacific sector of the Southern Ocean. Geochim. Cosmochim. Acta 79, 41-59.

Foster, G.L., Vance, D., Prytulak, J., 2007. No change in the neodymium isotope composition of deep water exported from the North Atlantic on glacial-interglacial time scales. Geology 35, 37–40.

German, C.R., Masuzawa, T., Greaves, M.J., Elderfield, H., Edmond, J.M., 1995. Dissolved rare earth elements in the Southern Ocean: Cerium oxidation and the influence of hydrography. Geochim. Cosmochim. Acta 59, 1551–1558.

Goldstein, S.J., Jacobsen, S.B., (1987). The Nd and Sr isotopic systematics of river-water dissolved material: implications for the sources of Nd and Sr in seawater. Chem. Geol. (Isot. Geosci. Sect.)66, 245-272.

Lacan, F., Jeandel, C., 2001. Tracing Papua New Guinea imprint on the central Equatorial Pacific Ocean using neodymium isotopic compositions and Rare Earth Element patterns. Earth Planet. Sci. Lett. 186, 497–512.

Locarnini, R.A., Mishonov, A.V.,Antonov, J.I.,Boyer, T.P., Garcia, H.E.,Baranova, O.K.,Zweng, M.M.,Johnson, D.R., 2010. World Ocean Atlas 2009, Volume 1: Temperature.S. Levitus, Ed. NOAA Atlas NESDIS 68, U.S. Government Printing Office, Washington, D.C., 184 pp.

Pahnke, K., Goldstein, S.L., Hemming, S.R., 2008. Abrupt changes in Antarctic Intermediate Water circulation over the past 25,000 years. Nature Geosci. 1, 870–874.

Pena, L.D., Calvo, E., Cacho, I., Eggins, S., Pelejero, C., 2005. Identification and removal of Mn-Mg-rich contaminant phases on foraminiferal tests: Implications for Mg/Ca past temperature reconstructions. Geochem. Geophys. Geosyst. 6, doi:10.1029/2005GC000930.

Pena, L.D., Cacho, I., Calvo, E., Pelejero, C., Eggins, S., Sadekov, A., 2008b. Characterization of contaminant phases in foraminifera carbonates by electron microprobe mapping. Geochem. Geophys. Geosyst 9, Q07012, doi:10.1029/2008GC002018.

Piepgras, D.J., Wasserburg, G.J., 1980. Neodymium isotopic variations in seawater. Earth Planet. Sci. Lett. 50, 128–138.

Piepgras, D.J., Wasserburg, G.J., 1982. Isotopic composition of neodymium in waters from the Drake Passage.Science 217, 207–214.

Piepgras, D.J., Wasserburg, G.J., 1987. Rare earth element transport in the western North Atlantic inferred from Nd isotopic observations. Geochim. Cosmochim. Acta 51, 1257–1271.

Piepgras, D.J., Jacobsen, S.B., 1988. The isotopic composition of neodymium in the North Pacific.Geochim. Cosmochim. Acta 52, 1373–1381.

Rosenthal, Y., Lam, P., Boyle, E.A., Thomson, J., 1995. Authigenic cadmium enrichments in suboxic sediments: Precipitation and postdepositional mobility. Earth Planet. Sci. Lett. 132, 99–111.

Rutberg, R.L., Hemming, S.R., Goldstein, S.L., 2000. Reduced North Atlantic Deep Water flux to the glacial Southern Ocean inferred from neodymium isotope ratios. Nature 405, 935–938.

Tanakawa, T., Togashi, S., Kamioka, H., Amakawa, H., Kagami, H., Hamamoto, T., Yuhara, M., Orihashi, Y., Yoneda, S., Shimizu, H., Kunimaru, T., Takahashi, K., Yanagi, T., Nakano, T., Fujimaki, H., Shinjo, R., Asahara, Y., Tanimizu, M., Dragusanu, C., 2000. JNdi-1: a neodymium isotopic reference in consistency with LaJolla neodymium. Chemical Geology 168, 279–281.

van de Flierdt, T., Robinson, L.F., Adkins, J.F., Hemming, S.R., Goldstein, S.L., 2006. Temporal stability of the neodymium isotope signature of the Holocene to glacial North Atlantic.Paleoceanography 21, PA4102, doi:10.1029/2006PA001294.

Xie, R.C., Marcantonio, F., Schmidt, M.W., 2012.Deglacial variability of Antarctic Intermediate Water penetration into the North Atlantic from authigenic neodymium isotope